Transparent Macroporous Polymer Monoliths

J. H. G. Steinke,† I. R. Dunkin, and D. C. Sherrington*

Department of Pure and Applied Chemistry, University of Strathclyde, Thomas Graham Building, 295 Cathedral Street, Glasgow G1 1XL, Scotland, U.K.

Received December 19, 1995; Revised Manuscript Received June 12, 1996[⊗]

ABSTRACT: Free-radical polymerization of trimethylolpropane trimethacrylate (TRIM) was carried out in the presence of a variety of porogens at room temperature, yielding transparent (macro)porous polymer monoliths. N_2 BET and surface area and Hg intrusion porosimetry data from the resulting polymers showed a variety of different pore sizes and pore size distributions. In the latter, three distinct maxima at 13, 50−60, and ∼500 nm were found for small pores (<500 nm) whereas the observed pore size maxima for large pores (>500 nm) did not exhibit any regularity. Variation of initiator concentration, ratio of monomer to porogen, polymerization temperature, and cross-linker had no influence in obtaining transparent monoliths. Correlation of the transparency of the monoliths with the refractive index and solubility parameter of the corresponding porogens led to threshold values for the refractive index (1.42) above which, and for the total solubility parameter (∼20 $(MPa)^{1/2}$) below which, a transparent polymer monolith is generally obtained, if one allows for exceptions. A correlation between pore size distribution and transparency, however, could not be found.

Introduction

Thin films,[1] liquid crystals,[2] multiphase polymer composites,[3] xerogels,[4] glass fibers,[5] and organic−inorganic glasses[6] are prominent examples of polymers whose potential areas of application (window insulation,[4] film coatings,[1] photo[7]- and electrochromic[8] devices, photo[9]- and electroluminescent[10] displays, LC displays,[11] and optical sensors[12]) require materials with high optical transparency and thus the optical properties of these polymers have been studied extensively.

In contrast to the wealth of information available on optical properties of polymers prepared by the sol−gel process,[13−15] only little is known about their organic counterparts, i.e., highly cross-linked polymer networks based on multifunctional cross-linkers such as divinylbenzene (DVB) or ethylene dimethacrylate (EDMA).

This is somewhat surprising, in particular when considering the structural similarites between macroporous polymer networks, e.g., poly(HIPE) on the one hand[16] and porous silica on the other.[4] In both cases a high degree of control over the pore structure (pore size, pore size distribution, shape of pores, and pore volume) can be achieved. Both types of polymeric networks suffer from becoming brittle upon drying. In both cases this problem is overcome by the right choice of "co-network" (IPN).[6,17]

Obviously, porous silica networks exhibit higher thermal stability compared to carbon-based polymers. An advantage of porous organic networks on the other hand is the facile introduction of a wide variety of functional groups either via suitably chosen comonomers or via polymer-analogue functionalizations carried out as a postmodification step. Control of both, pore structure and functionalities within the pores, in combination with optical clarity, could be of interest for a number of reasons. Photochemical reactions taking place within the pores would present a novel approach of carrying out synthetic transformations in a defined (restricted) reaction space. So far, zeolites, container compounds, micelles, and dendrimers have been studied toward this goal, none of which offers much flexibility and control over pore structure and the presence of functional groups.[18] Furthermore, a transparent monolith could be used to study the chromatographic process[19] in real time by UV−vis spectroscopy or any other analytical technique requiring optically transparent conditions. Up to now, this has only been done either indirectly, by using fluorescent dyes as indicators,[20] or directly by NMR spectroscopy,[21] which lacks sensitivity and its time scale is slow compared to optical techniques. It is even conceivable to use chemically selective transparent monoliths, obtained through molecular imprinting for example, as optical sensors offering all the advantages associated with optical spectroscopy.[22]

The lack of studies concerned with the optical properties of (macro)porous polymer networks and our interest in designing novel optical sensors prepared using the concept of molecular imprinting led us to investigate the synthesis of transparent (macro)porous polymer monoliths in more detail. The results of this study have already enabled us to synthesize selective, transparent polymer monoliths. These monoliths have been turned into anisotropic networks by performing a photoselective reaction on the polymer itself. The underlying concept and the synthesis have been reported elsewhere.[22]

Here we should like to present our efforts in the syntheses of transparent polymer monoliths with controlled pore structures based on trimethylolpropane trimethacrylate (TRIM).

Experimental Section

Chemicals. All solvents used in polymerizations were purified and dried according to standard procedures. They were stored under argon and were kept over dried molecular sieves (4 Å). Trimethylolpropane trimethacrylate (TRIM) of technical quality (90%) and ethylene dimethacrylate (EDMA, 98%), were obtained from Aldrich Chemical Co. Ltd., and each compound was fractionally distilled prior to use. Azobis(isobutyronitrile) (AIBN) and azobis(2,4-dimethylvaleronitrile) (ADVN) were of analytical grade. 2-Acrylamido-2-methylpropanesulfonic acid (AMPSA, 99%) was obtained from Aldrich, recrystallized twice from a mixture of ethanol and water, and dried over P_2O_5 under vacuum. Michler's ketone (MK, 98%), supplied by Aldrich Chemical Co. Ltd., was recrystallized twice from ethanol/toluene and subsequently at least twice from pure ethanol. It was dried over P_2O_5 under vacuum.

* To whom correspondence should be addressed.
† Current address: Melville Laboratory for Polymer Synthesis, Department of Chemistry, University of Cambridge, Pembroke Street, Cambridge CB2 3RA, UK.
⊗ Abstract published in *Advance ACS Abstracts,* July 15, 1996.

S0024-9297(95)01875-4 CCC: $12.00

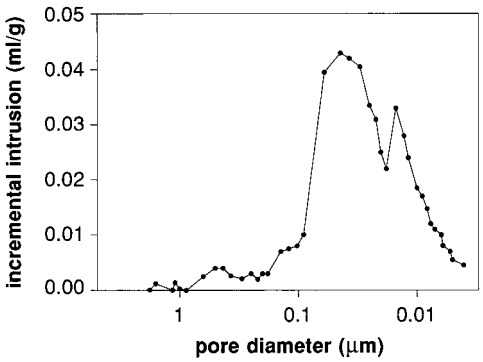

Figure 1. Plot of incremental intrusion versus pore diameter for T1 from Hg porosimetry data.

Polymerization. The compositions of the monomer mixtures are summarized in Tables 1, 3, 5, and 7. Standard compositions consisted of a monomer to porogen ratio of 30:70 (v/v) and 1 mol % of free-radical initiator (to monomer). The preparation of the polymer monoliths was carried out as follows. The initiator was weighed into a polymerization ampule. The ampule was evacuated, filled with nitrogen, and sealed before placing it just above the surface of a dry ice/ethanol slush. Cross-linker and monomers were added next, and then the porogen. A stream of dry nitrogen was bubbled through the polymerization mixture for 10 min. The ampule was immersed into the slush, and nitrogen bubbling was discontinued after another 5 min. The polymerization tube was thereafter immersed in liquid nitrogen. Three freeze–pump–thaw cycles were carried out under vacuum. After the last cycle, the ampule, which was still under vacuum, was sealed and left to warm to room temperature. The polymerization mixture was homogenized and finally polymerized and cured for a specified time and temperature (see Tables 1, 3, 5, and 7).

Post-treatment. The polymers were dried inside the ampule under reduced pressure at a specified temperature and for a specified period of time (see Tables 1, 3, 5, and 7). They were then ground, and the bed volume of the polymers was measured using calibrated tubes, first in the dry and then in the swollen state, allowing at lesat 72 h to reach equilibrium conditions with occasional agitation of the gels during this period of time.

Texture Determination. The pore structure for a pore radius larger than 3 nm was determined by mercury porosimetry[23] using pressure of up to 450 MPa (Micromeritics 9220). A typical pore size distribution profile (for polymer T1) is shown in Figure 1. The surface area was obtained from adsorption measurements with nitrogen according to the BET method (Micromeritics Accusorb 2100E).[24] Polymer samples were degassed in their sample holders overnight at 60 °C. Porosimetry and BET data are summarized in Tables 2, 4, 6, and 8.

Texture Calculations. Percentage values of pore size contributions for pores smaller than 10 000 nm were calculated from their corresponding pore volume (excluding any pore volume found for pore sizes greater than 10 000 nm).

Transparency Assessment. The optical quality (turbidity) of polymer monoliths was assessed after polymerization and curing of the polymer network had taken place. For this purpose, written text was viewed through the polymer sample (about 1.5 cm diameter). A polymer monolith, through which printed letters appeared essentially undistorted and clear was classified as transparent. If images became distorted and weaker but were still recognizable when viewed through a polymer, it was then classified as translucent. Polymer samples that did not allow any pattern at all to be discerned were categorized as opaque. In order to be able to plot physical data versus the optical appearance (turbidity) of each polymer monolith, transparent polymers were set arbitrarily to 1, translucent polymers to 0.5, and opaque monoliths were given the value 0.

Determination of Unreacted Carbon–Carbon Double Bonds. The amount of unreacted methacrylate groups was determined by solid-state ^{13}C-CP-MAS NMR spectroscopy on a 25 MHz Bruker MSL-100 solid-state spectrometer.[25] The spectra were obtained by using approximately 200 mg of sample packed in a zirconia rotor, sealed with a KEL-F endcap and spun at ca. 5000 Hz. The recycle delay between each pulse was 1.5 s and the CP contact time was 1 ms. For all spectra the chemical shifts were externally referenced to TMS (0.0 ppm).

Results and Discussion

Few publications are available which mention transparent and macroporous polymers. Transparency is achieved usually by refractive index matching. Damen and Neckers[26] added a molecularly imprinted porous styrene–divinylbenzene copolymer to a benzene solution and carried out a photochemically allowed dimerization reaction. Although they did not explicitly mention the transparent nature of the suspension, it can be assumed that benzene matched the refractive index of the macroporous polymer. Similarly, Wulff and Kirstein[27] measured the optical rotation of chiral cavities in a highly cross-linked macroporous polymer. A blend of 1,2-dichloroethane, tetrachloroethylene, and *o*-dichlorobenzene ensured transparency although the polymer was prepared initially by using tetrahydrofuran (THF) as pore-forming agent. Mosbach et al.[28] initiated the polymerization of methacrylate monomers at 4 °C photochemically at 366 nm. One has to assume either that the swollen polymer stayed transparent throughout the polymerization or that until gelation occurred a sufficient number of radicals are formed to guarantee the further formation of the polymer network.

Detailed investigations into the pore structure and accessibility of highly cross-linked macroporous poly(meth)acrylamides by Shea et al.[29] showed that macroporosity depended strongly on porogen and cross-linker. Fluorescence labeling experiments, suggesting the presence of transparent polymer networks, revealed the macroporous polymers to be more permeable to polar solvents than to nonpolar ones. However, differences in the transparency due to choice of cross-linker, cross-linker concentration, or porogen have not been stated explicitly.

A paper by Rosenberg and Flodin in 1987 is probably the first, among only a few, in which the authors in fact mention a transparent macroporous polymer.[30] The effect of the porogen on the microstructure of a highly cross-linked TRIM polymer was studied. It was found that transparent polymers were encountered when the solubility parameter of the porogen exceeded a threshold value of 19.4 $(MPa)^{1/2}$. Furthermore, they established that no macroporosity was introduced when the solubility parameters of polymer and porogen differed too much from each other.

This was the background on which we based our study. Our initial goal was to explore compositions and reaction conditions which would allow us to synthesize transparent polymers with defined morphology as part of a concept leading to novel optical sensors.[22] However, the subject became interesting in its own right, and so we set out to elucidate relationships between transparency and morphology of these polymer monoliths.

Polymer monoliths were prepared by precipitation polymerization at room temperature. For comparison, a small number of polymers were also prepared at 60 °C. Classification of the polymer monoliths into three categories (transparent, translucent, and opaque) was regarded as being sufficient, because for the final application in mind, only a truly transparent polymer

Table 1. Compositions and Reaction Conditions for TRIM and EDMA Polymers (T1−T19) Obtained in the Presence of Different Porogens[a]

polymer code	solvent/mL	cross-linker/mL	polymerization t (h)/T (°C)	curing t (h)/T (°C)	optical appearance
T1	toluene/3.50	TRIM/1.50	16/20	24/60	transp
T2	toluene/3.50	TRIM/1.50	20/60	16/60	transp
T3	toluene/4.60	EDMA/2.00	20/60	16/60	transp
T4	$CHCl_3$/3.50	TRIM/1.50	20/20	16/60	transp
T5	HCO_2Et/3.50	TRIM/1.50	20/20	20/60	opaque
T6	PhCl/3.50	TRIM/1.50	20/20	16/70	transp
T7	PhCl/3.50	EDMA/1.50	20/20	16/70	transp
T8	PhCl/3.50	TRIM/1.50	20/60	16/70	transp
T9	PhCl/3.50	EDMA/1.50	20/60	16/70	transp
T10	acetone/3.50	TRIM/1.50	24/20	16/60	opaque
T11	CH_2Cl_2/3.50	TRIM/1.50	72/20	16/60	transp
T12	$C_6H_{10}O$/3.50	TRIM/1.50	72/20	16/70	transl
T13	$(CH_2Cl)_2$/3.50	TRIM/1.50	24/20	16/60	transp
T14	AcCN/3.50	TRIM/1.50	48/20	16/60	opaque
T15	MeOH/3.50	TRIM/1.50	24/20	16/60	opaque
T16	DMSO/3.50	TRIM/1.50	24/20	16/55	opaque
T17	NMP/3.50	TRIM/1.50	24/20	16/55	transp
T18	DMAc/3.50	TRIM/1.50	24/20	16/55	transl
T19 (E1)	NMP:$CHCl_3$/0.50:1.80	TRIM/2.30	24/20	16/60	transp

[a] AIBN is used as free-radical initiator for polymerizations carried out at 60 °C, ADVN at 20 °C.

Table 2. Hg Porosimetry and N_2 Adsorption (BET) Data for Polymers T1−T19[a]

polymer code	area ($m^2\ g^{-1}$)	vol (mL g^{-1})	bulk (g mL^{-1})	skeletal (g mL^{-1})	s/b	pore ϕ (nm)	pore max (nm)	pore >500 nm	surf area ($m^2\ g^{-1}$)
T1	168.3	0.67	0.68	1.25	1.84	7.7	13/50/500	yes	472
T2	90.3	0.52	0.64	0.96	1.50	7.5	13/50/500	yes	214
T3	146.2	1.02	0.57	1.35	2.38	7.5	13/60/500	yes	381
T4	38.2	0.57	0.56	0.82	1.47	4.9	13/50/500	YES	nd
T5	4.9	0.48	0.61	0.87	1.42	4.4	<10	yes	nd
T6	28.2	0.59	0.79	1.50	1.89	4.6	7/13/500	yes	1.2
T7	84.7	0.53	0.63	1.28	2.03	7.2	13/50/500	yes	309
T8	111.4	1.28	0.43	0.94	2.20	5.4	13/60/500	YES	nd
T9	94.4	0.83	0.63	1.32	2.10	8.1	13/50/500	YES	346
T10	nd	nd	nd	nd	nd	nd	nd	nd	nd
T11	51.9	0.41	0.78	1.15	1.48	4.7	13/60/500	yes	0
T12	36.0	0.25	0.93	1.21	1.30	4.6	13/50/500	yes	0.3
T13	31.1	0.53	0.75	1.23	1.66	4.6	14/50/500	YES	1.0
T14	45.3	0.25	0.69	0.84	1.21	7.1	12/40/130	yes	nd
T15	51.7	1.45	0.45	1.28	2.86	5.2	13/60/130	YES	16
T16	0.0	0.08	0.71	0.76	1.06	*	*/*/*	yes	429
T17	0.8	0.19	0.73	0.85	1.16	4.2	11	YES	343
T18	128.9	0.35	0.85	1.21	1.43	7.2	11/15/30	no	380
T19	42.0	0.15	1.31	1.62	1.24	6.0	13/60/450	YES	0.3

[a] The values for "surf area" were determined by N_2 adsorption measurements; all other data were obtained by Hg porosimetry. The pore size maxima have been divided into pores larger and smaller than 500 nm. For pore sizes equal to or smaller than 500 nm, the biggest maximum is underlined. If pore sizes greater than 500 nm do contribute to the total pore volume, a small "yes" is used. If in addition to this, the global maximum within the pore size distribution is found for pore sizes greater than 500 nm, a capital "YES" is used. Otherwise the underlined pore size maximum represents the global pore size maximum, "area": pore area; "volume": pore volume; "bulk": bulk density; "skeletal": skeletal density; s/b: ratio of skeletal to bulk density; "pore ϕ": mean pore diameter; "pore max": pore size maximum for pores smaller than 500 nm; "pore > 500 nm": pore size maximum indicator for pores larger than 500 nm; "surf area": surface area (BET). Note: * indicates no significant contribution to the pore volume for pore sizes smaller than 5000 nm.

could be considered. Depending on the porogen used, the mechanical stability of the polymers varied from brittle in shear (usually high surface area) to hard and glassy (usually low surface area), although all showed good rigidity in compression.

Influence of Porogen (Polymers T1, T4−T6, and T10−T19). The choice of porogen was intended to cover a wide range of solvents from polar species such as methanol to relatively nonpolar ones such as toluene. A change of porogen had the most pronounced effect on transparency and morphology of the TRIM- and EDMA-based polymers. Data on the optical appearance of these polymers are summarized in Tables 1 and 2. Figure 2 shows the plot of transparency of the polymer monolith versus refractive index of the corresponding porogen. Transparent polymers are observed for porogens with a refractive index higher than 1.42 and opaque polymers below this threshold. However, dimethyl sulfoxide (DMSO) with a refractive index of 1.475 also gives an opaque polymer, and two other porogens, cyclohexanone and dimethylacetamide (DMAc), which also have refractive indices higher than 1.42, yielded translucent polymers. A very similar observation concerning a threshold value for the refractive index was made by Sellergren and Shea.[31] While their main objective was to study the influence of polymer morphology on the ability to resolve enantiomers using molecularly imprinted highly cross-linked networks (80 mol % EDMA), they found that "depending on which porogen was used either transparent, translucent, or opaque polymers were obtained..." and concluded "that the transparent polymers were prepared using porogens with a refractive index higher than 1.40". Unfortunately, their study did not include the porogens that we found not to follow this general trend. Nevertheless, both observations clearly indicate that a strong mis-

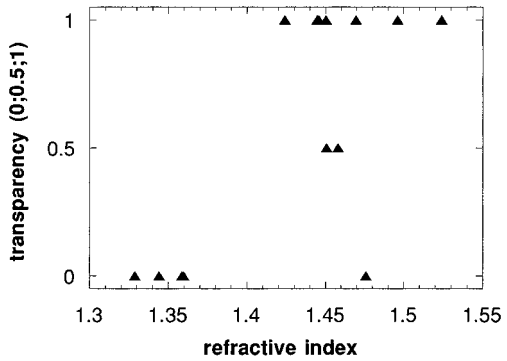

Figure 2. Plot of refractive index of the porogens against the transparency of the corresponding polymer monolith (polymers T1−T19).

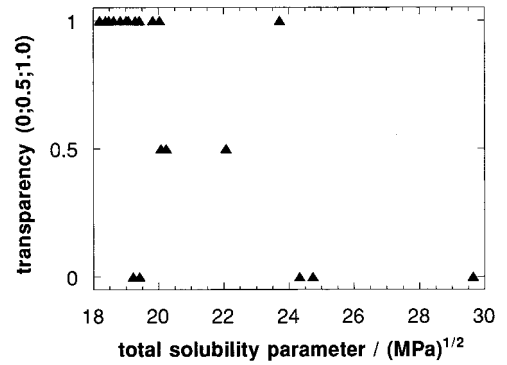

Figure 3. Plot of the total solubility parameter of the porogen versus the transparency of the corresponding polymer monolith for polymers T1−T19 and S1−S9.

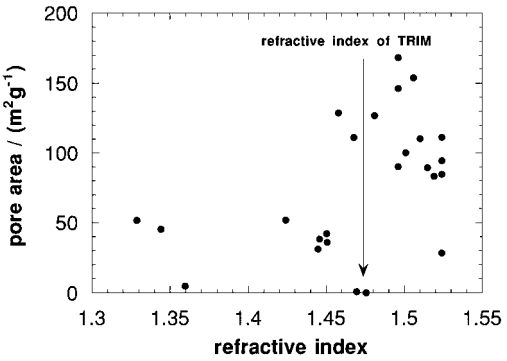

Figure 4. Refractive index of the porogen plotted against the pore area (Hg porosimetry) of the corresponding polymer monolith (polymers T1−T19 and S1−S9).

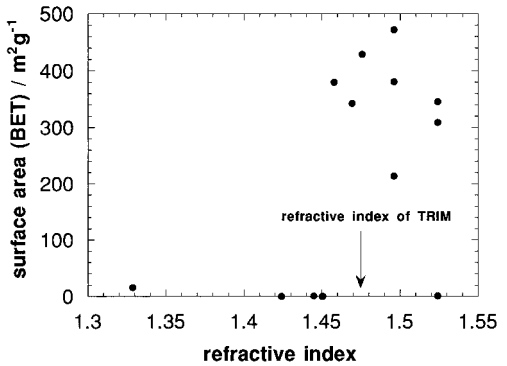

Figure 5. Plot of refractive index of porogen versus surface area of the corresponding polymer monolith as measured by BET for polymers T1−T19 and S1−S9.

match in refractive indices between porogen and polymer will lead to a loss in transparency.

A plot of turbidity of the polymer monoliths versus the total solubility parameter (δ_{sum} $(MPa)^{1/2}$) of the porogen used (Figure 3) shows that porogens with $\delta_{sum} < 20.4$ $(MPa)^{1/2}$ yield transparent polymers (exceptions: ethyl formate, acetone, and cyclohexanone) and those with $\delta_{sum} > 20.4$ $(MPa)^{1/2}$ lead to translucent or opaque polymers (exception: *N*-methylpyrrolidone (NMP)). A plot of turbidity against the dispersion force contribution of the total solubility parameter (not shown) exhibits a threshold value (also similar in correlation) to that found in Figure 3. Above 16.6 $(MPa)^{1/2}$ the monoliths become transparent with the exceptions of the porogens cyclohexanone, DMSO, and DMAc. Plots of turbidity versus polar contributions or hydrogen-bonding contributions showed much weaker correlations (not shown). These results contrast with those of Rosenberg and Flodin (vide infra), who found transparent poly(TRIM) monoliths for porogens whose total solubility parameters are greater than 19.4 $(MPa)^{1/2}$. However, of the seven solvents used in their study, only two qualified, having a total solubility parameter greater than the threshold value.

The surface area obtained from N_2 adsorption measurements varied from 0 to 472 m^2 g^{-1}. Pore areas determined by mercury porosimetry covered the range of 0−168 m^2 g^{-1}. Pore volumes also varied widely from 0.072 up to 1.45 mL g^{-1}. The mean pore diameter covered the interval of 4.2−16.8 nm. Care is required in interpreting Hg porosimetry data at high pressures, and, in this work, corresponding low values for the mean pore diameters. However, since all the polymer monoliths displayed good bulk rigidity, use of the pore diameter data at face value seems reasonable. Skeletal densities were found to lie between 1.62 and 0.47 g mL^{-1}, and bulk densities ranged from 0.42 to 1.30 g mL^{-1} (Table 2). These data ranges give a first good impression how widely the morphology of these transparent (macro)porous polymers differ due to the influence of the porogen. The pore size distribution was of particular interest. It was hoped that transparent and nontransparent polymers would differ in the frequency of their pore sizes. However, this was not observed. Almost all polymers possess three pore size maxima at or below 500 nm and at least one above this value (Table 2). Most commonly encountered were maxima at about 500, 60−50, and 13 nm. In some cases, the maximum at 500 nm was replaced by a maximum at about 130 nm. These maxima were further distinguished by their size (Table 2). Most frequently the maximum at 13 nm represents the absolute maximum for pore sizes but absolute maxima for 60−50, 500, and above 500 nm were also observed. *A trend which would link the pattern of pore size maxima with transparency or any other porosimetry parameter does not, however, emerge.* Attempts were also made to correlate polymer porosimetry data (including BET) and the transparency of the polymer monoliths to the refractive index and solubility parameters of the porogens used in the preparation of the corresponding polymer networks. The refractive index of each porogen is plotted against the pore area of the corresponding polymer in Figure 4. Although the data are scattered, a maximum is apparent for $n \sim 1.5$. Although this cannot be related unambiguously to the refractive index of TRIM, which is 1.4720, the correspondence is close. A similar trend is seen in the surface area (BET) data (Figure 5).

Solid-state NMR spectra (^{13}C-CP-MAS) were recorded for a small number of samples. The amount of unreacted double bond was calculated from the peak areas

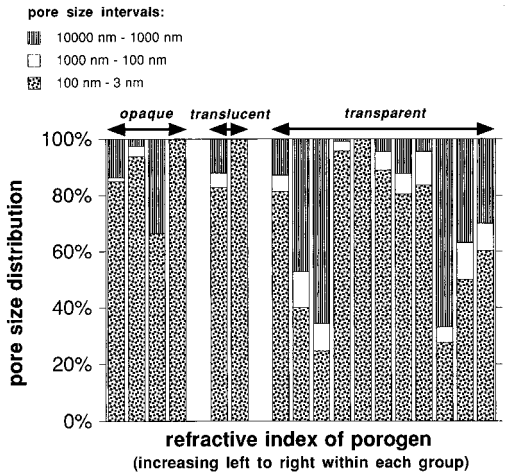

Figure 6. Graphic representation of the contribution of different pore size intervals toward the total pore volume of polymers T1−T19.

of the two carbonyl groups present and was about 10% in all cases. The ^{13}C NMR spectra were in excellent agreement with poly(TRIM) spectra by Hjertberg et al.[25] and Rosenberg et al.;[30] however a trend that would link ^{13}C NMR spectra and observed transparency of the polymers did not emerge.

Whether a correlation between transparency and pore structure exists was also investigated. This was pursued by grouping together opaque, translucent, and transparent polymers and correlating pore size distribution with the refractive index of the porogen (Figure 6). Distributions are expressed as a percent pore volume contribution within the intervals 10 000−1000, 1000−100, and 100−3 nm. The reason for this kind of treatment of the data arose from the idea that it might be possible to find a link between opaque polymers and the contribution of pores which are of similar size to the wavelength of light. Larger pores were included because theoretical calculations based on the Mie theory[32] of light scattering[33,34] predict that their contribution to light scattering is small but not negligible. Smaller pores are included for the same reason but also because Hg porosimetry and N_2 adsorption characterize the polymer in its *dry* state. Transparency is judged, however, in the swollen state. Flodin et al.[35] compared dry-state techniques with swollen-state techniques, such as size exclusion chromatography (SEC). To correlate pore sizes and pore size distributions between the swollen and the dry states, the shape of pores was approximated to spherical and pore sizes of the swollen state were therefore calculated by multiplication of the pore size in the dry state by the swelling factor to the power of $^1/_3$ (pore size swollen = pore size dry × (swelling factor)$^{1/3}$). It was shown that the calculated data were in good agreement with the results obtained from porosimetry measurements. With a swelling factor of about 2 for the polymers in the present investigation, it was therefore important to include dry pore sizes from 300 down to 100 nm, since, once swollen, these may reach a size similar to the wavelength of light.

It can be seen from Figure 6 that the main contribution toward the overall pore volume in most polymers arises from the smallest pores (<100 nm) and hence will not contribute to light scattering. This means that transparency is not influenced significantly by the contribution of pores in the interval of 1000−100 nm. The maximum contribution of these pores is about 12%. If one considers only the pore size interval 700−300 nm, then this value drops to 8%. Most polymers in fact show values which are significantly less. Such a low contribution from pore sizes corresponding to visible light wavelengths is not sufficient to introduce enough scattering of light to make a polymer appear opaque or translucent.[33,34] An explanation for the observed behavior is not therefore at hand at the moment.

Table 3. Compositions and Reaction Conditions for TRIM Polymers (S1−S9) Obtained in the Presence of Different Porogens[a]

polymer code	solvent 1/mL	solvent 2/mL	curing t (h)/T (°C)	optical appearance
S1	PhCl/3.50		16/70	transp
S2	PhCl/2.87	toluene/0.63	15/60	transp
S3	PhCl/2.30	toluene/1.20	15/60	transp
S4	PhCl/1.72	toluene/1.78	15/60	transp
S5	PhCl/1.15	toluene/2.35	15/60	transp
S6	PhCl/0.57	toluene/2.93	15/60	transp
S7	$CHCl_3$/0.86	toluene/2.64	16/70	transp
S8	$CHCl_3$/1.73	toluene/1.77	16/70	transp
S9		toluene/3.50	16/70	transp

[a] Conditions: TRIM = 1.50 mL; polymerization time/temperature = 20 h/20 °C; radical initiator ADVN.

Influence of Porogen Combination (Polymers S1−S6 and S9). These polymers were prepared by a stepwise change of the composition of the porogen from pure chlorobenzene to pure toluene (Table 3) (both porogens used separately lead to transparent monoliths). The ratio of cross-linker to porogen mixture was kept constant throughout (30:70 (v/v); cross-linker: porogen). All polymers obtained were transparent. When the pore area of polymers S1−S6 and S9 is plotted against the total solubility parameter of the corresponding porogen (not shown), a trend emerges that with increasing concentration of chlorobenzene in the porogen mixture the pore area decreases. Only polymer S6 (Table 4) deviates strongly from this trend. Changes in pore volume and mean pore diameter also follow the same trend with the exception of polymer S1, which shows a higher value for its pore volume. BET data of these polymers plotted against the total solubility parameter of the porogen mixture show a rather peculiar behavior (Figure 7). The surface area is relatively low for volume ratios of toluene to chlorobenzene up to a ratio of 1:1 (v/v), about 20−30 $m^2\ g^{-1}$, but rises sharply once toluene is present in excess (2:1 (v/v)) and increases further with increasing concentration of toluene in the porogen mixture. This sudden change is not manifest in the porosimetry data (Table 4), but the same general trend is apparent.

The volume contribution of pore sizes between 700 and 300 nm never exceeds 4% of the total pore volume and the maximum pore volume found for the extended interval 1000−100 nm is about 13%. This of course explains why all polymers of this series are transparent. The overall contribution from the volume of pore sizes between 1000 and 100 nm is hardly affected by the change in porogen composition (except S6), nor is any trend observed between the solubility parameter and contribution of pore sizes within this interval.

These results differ from those of Rosenberg et al.[30] All of the polymers in this series are prepared using a porogen mixture with a refractive index which is below the threshold of 19.4 $(MPa)^{1/2}$ found by Rosenberg et al. Furthermore, we have obtained transparent polymers with toluene as porogen (18.2 $(MPa)^{1/2}$), contrary to the findings in their paper. Interestingly, both sets of polymer samples possess a very similar pore structure as indicated by porosimetry and surface area data.

Table 4. Hg Porosimetry and N_2 Adsorption (BET) Data for Polymers S1−S9 (See Footnote *a* of Table 2)

polymer code	area ($m^2\ g^{-1}$)	volume ($mL\ g^{-1}$)	bulk ($g\ mL^{-1}$)	skeletal ($g\ mL^{-1}$)	*s*/*b*	pore ϕ (nm)	pore max (nm)	pore >500 nm	surf area ($m^2\ g^{-1}$)
S1	28.2	0.59	0.79	1.51	1.89	4.6	7/13/500	yes	1.2
S2	83.3	0.29	0.88	1.18	1.34	6.4	13/50/130	no	32
S3	89.4	0.32	0.87	1.21	1.39	6.2	13/50/130	yes	20
S4	110.4	0.34	0.81	1.12	1.38	5.8	13/50/130	no	16
S5	154.1	0.41	0.78	1.14	1.46	7.4	13/50/450	yes	393
S6	100.4	0.69	0.60	1.04	1.72	16.8	13/60/500	yes	444
S7	126.9	0.44	0.86	1.39	1.61	6.4	13/50/500	yes	nd
S8	111.2	0.24	0.87	1.11	1.27	5.8	13/50/120	no	nd
S9	168.3	0.67	0.68	1.25	1.84	7.7	13/50/500	yes	nd

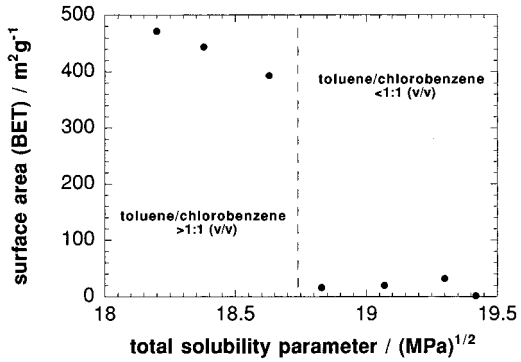

Figure 7. Plot of total solubility parameter of the porogen versus surface area of the corresponding polymer monolith as determined by BET for polymers S1−S6 and S9.

A full comparison, however, is not possible because we did not conduct BET measurements to determine pore size distributions below 3 nm, owing to our focus on pores similar in size to the wavelength of light. In addition, our polymers were synthesized at room temperature using a more reactive free-radical initiator (ADVN), whereas Rosenberg et al. employed AIBN at 70 °C.

Influence of Cross-Linker Structure (Polymers T2, T3, T6, and T7). The effect of changing the cross-linker from TRIM to EDMA on the porosity and transparency of polymers prepared in the presence of either toluene or chlorobenzene at 20 and 60 °C was also studied (Table 1). All polymers obtained were transparent. Polymer monoliths prepared in toluene based on TRIM (T2) or EDMA (T3) showed macroporous morphology and high surface areas in both cases (Table 2). The changes of characteristic morphology data were dramatic in some cases. The pore volume (Hg intrusion) and surface area (BET) are doubled for the polymer monolith where TRIM (T2) was replaced by EDMA (T3). Pore area and skeletal density increased by about 60%, and bulk density showed a slight decrease. The mean pore diameter stayed unchanged. Pore size maxima were observed at 500, 60−50, and 13 nm. The absolute pore size maximum however moved from 13 (TRIM) to 60 nm (EDMA). Polymers T6 and T7 are only different from T2 and T3 in that the porogen was changed from toluene to chlorobenzene (Table 1). However, a drastic increase in surface area (BET) was observed when the cross-linker was changed from TRIM (1.2 $m^2\ g^{-1}$; T6) to EDMA (390 $m^2\ g^{-1}$; T7). This was also reflected in a threefold increase of pore area (Hg intrusion) (Table 2). The mean pore diameter increased from 4.6 (T6) to 7.2 nm (T7) and the absolute pore size maximum moved from 500 nm for T6 to 13 nm in the case of T7.

The relatively small structural change in the chosen cross-linker (TRIM for polymers T2 and T6; EDMA for polymers T3 and T7) did not affect the transparency of the polymers. The pore size distribution pattern is not influenced to any significant degree. Transparency is also independent from the choice of porogen (toluene or chlorobenzene) and the polymerization temperature (20 or 60 °C). However, the number of samples studied is too small to allow more general conclusions to be drawn.

Table 5. Compositions and Reaction Conditions for TRIM Polymers (C1−C4) Obtained Using Different Ratios of Cross-Linker to Porogen[a]

polymer code	solvent (S)/ mL	ratio S/C (v/v)	optical appearance
C1	PhCl/4.50	60/40	transp
C2	PhCl/3.00	50/50	transp
C3	PhCl/2.00	40/60	transp
C4	PhCl/1.30	30/70	transp

[a] Conditions: TRIM (C) = 3.00 mL; polymerization time/temperature = 23 h/20 °C; curing time/temperature = 2 h/60 °C.

Influence of Porogen/Cross-Linker Ratio (Polymers C1−C4). A series of TRIM-based polymers were prepared with chlorobenzene as the porogen (Table 5). The ratio of porogen to cross-linker was varied in steps of 10% from 60:40 to 30:70 (v/v) (C1−C4). All polymers were obtained as transparent macroporous monoliths. Data on their morphology are shown in Table 6. The changes in all the porosimetry parameters are rather small but concur with observations made in the literature for styrene−divinylbenzene resins by Millar et al.[36] Overall, this porogen yields matrices with low surface areas (BET).

Influence of Initiator Concentration (Polymers IC1−IC4). TRIM was polymerized in the presence of toluene and chlorobenzene (2.5:1 v/v) with varying amounts of initiator ADVN (0.009−0.58 mmol, 0.2−12.3 mol % (IC1−IC4)) at room temperature (see Table 7). All polymers obtained were transparent. Porosimetry data suggest that the polymer morphology is little changed. Surface area does show some increase with increasing amount of initiator, although pore sizes gradually decrease (Table 8).

Influence of Polymerization Temperature (Polymers T6−T9). Polymers T6 and T8, and T7 and T9, are identical except for the temperature at which they were polymerized (Table 1). The latter were polymerized at 60 °C in the presence of AIBN, whereas the former were polymerized at 20 °C using ADVN as radical initiator. A less reactive initiator was chosen for the higher temperature in order to ensure that polymerization took place at a comparable rate. For the TRIM polymers, increasing the polymerization temperature increased the pore area, pore volume, and mean pore size and at the same time decreased the bulk and skeletal densities. Changes in polymer morphology were less pronounced with EDMA as cross-linker but the trends were similar. Again, all polymers obtained were transparent. In a recent paper by Sellergren and Shea,[31] the synthesis of EDMA polymer networks is reported either using an azo initiator at elevated tem-

Table 6. Hg Porosimetry and N_2 Adsorption (BET) Data for Polymers C1−C4 (See Footnote *a* of Table 2)

polymer code	area ($m^2\ g^{-1}$)	volume ($mL\ g^{-1}$)	bulk ($g\ mL^{-1}$)	skeletal ($g\ mL^{-1}$)	*s*/*b*	pore ϕ (nm)	pore max (nm)	pore >500 nm	surf area ($m^2\ g^{-1}$)
C1	62.7	0.22	0.99	1.27	1.27	6.0	13/50/130	yes	1.8
C2	57.8	0.20	0.99	1.23	1.24	6.0	13/60/130	yes	0.9
C3	51.6	0.20	1.03	1.30	1.27	5.6	13/50/130	yes	0.0
C4	40.3	0.21	1.00	1.27	1.26	4.9	13/60/120	yes	nd

Table 7. Compositions and Reaction Conditions for TRIM Polymers (IC1−IC4) Obtained Using Different Concentrations of Free-Radical Initiator to Monomer[a]

polymer code	solvent mL:mL	initiator mg/mmol	optical appearance
IC1	PhCl:tol 1.00:2.50	ADVN 2.0/0.009	transp
IC2	PhCl:tol 1.00:2.50	ADVN 5.4/0.025	transp
IC3	PhCl:tol 1.00:2.50	ADVN 23.8/0.11	transp
IC4	PhCl:tol 1.00:2.50	ADVN 128.0/0.58	transp

[a] Conditions: TRIM = 1.50 mL/4.7 mmol; polymerization time/temperature = 144 h/20 °C; curing time/temperature = 16 h/60 °C.

perature (60 °C) or a different, more reactive azo initiator at 15 °C, which was decomposed photochemically. THF as porogen led to a transparent polymer at the lower polymerization temperature, but an opaque polymer was obtained (using the same porogen) at 60 °C (Figure 8). The transparent polymer had a smaller surface area (BET), pore volume, pore diameter, micropore surface area (BET) and micropore volume compared to its opaque counterpart. Significant contribution of pore sizes above 300 nm were not reported. The presence or absence of pores of comparable size to the wavelength of light does not therefore account for the difference in turbidity observed with polymerization temperature. A tentative explanation is offered later.

Influence of Drying and Swelling. Upon evaporation of the porogen after polymerization, polymers with high surface area turn milky or opaque, and low surface area polymers stay clear. The degree of transparency of rewetted polymers was reduced relative to the original wet appearance in some cases, probably due only to light scattering at fractures produced in the matrix on drying, and not to any bulk effect.

Polymer T14, prepared in the presence of acetonitrile (Table 1), was dried and then swollen in chlorobenzene. The formerly opaque, dry polymer turned transparent with this change of medium. There was no obvious difference in transparency in the swollen polymer particles between T6, polymerized and swollen in chlorobenzene, and chlorobenzene-swollen T14. The porosimetry data on polymer T6 and T14 (Table 2) show major differences in pore volume, mean pore diameter, and skeletal density as well as pore size distribution and pore size maxima. The difference in refractive index between the porogens used is 0.18. Another representative case study is polymer T7. This was prepared in chlorobenzene and was swollen in chloroform after drying. Compared with the suspension of polymer particles of T7 in its original porogen, the presence of chloroform produced a less transparent suspension (difference in refractive indices between the two porogens = 0.05). Likewise polymer T8 showed a higher restoration of its transparency in its original porogen, chlorobenzene, than in NMP. The difference in refractive index is 0.05 in this case. This behavior can be explained by a better match of refractive indices between polymer and swelling agent. In the case of polymer T14 for example, the initial difference in refractive index is 0.13 for the combination of poly(TRIM) (assumed to be close to the refractive index of its monomer, TRIM) and acetonitrile. This difference is reduced to 0.05 by using chlorobenzene instead of acetonitrile as swelling agent. Both solvents are capable of swelling polymer T14 to a similar degree, so that one can assume that changes in pore structure are small. Therefore the difference in turbidity observed is not attributable to a change in the pore size distribution of the polymer network but to a closer match of refractive indices. While the latter is therefore clearly important, it is not the only factor.

Influence of Changing the Porogen in the Swollen State. For this purpose, polymer E1 was prepared as a monolith in a mixture of chloroform/NMP (3.7:1 v/v). In contrast to the composition of all other polymer monoliths, E1 contained 5 wt % of a 2.4:1 molar ratio of AMPSA to MK, giving the polymer a strong orange color in daylight. Irradiation at 254 nm however caused the polymer to fluoresce by emitting green light. The initial porogen mixture was changed gradually toward *n*-hexane over a 3 day period, leaving the transparency of the monolith unaffected apart from a hint of a milky appearance. The porogen was then changed back to more polar porogens, via chloroform and finally methanol (2 days in each case). The milky appearance disappeared and did not change when the porogen mixture became slowly richer in methanol. The polymer stayed transparent with a slight change of color from orange to red/orange. The sequence of solvent exchanges is shown in Scheme 1. The difference between the refractive indices of $CHCl_3$/NMP (3.7:1 v/v) and *n*-hexane is 0.07 and for $CHCl_3$/NMP (3.7:1 v/v) and methanol is 0.13. This obviously cannot be regarded as being a match of refractive indices, and it is remarkable that the polymer morphology allows this gap to be bridged.[33] As discussed in the previous section, a difference in refractive indices of 0.13 was sufficient to change a formerly opaque polymer into a transparent one. An explanation for the difference in behavior is not at hand at the moment. It is clear however that matching refractive indices between polymer and porogen is not the only parameter involved in producing (macro)porous transparent polymer monoliths.

Concluding Discussion

It has been shown that it is possible to prepare transparent polymers with very different morphologies in the presence of a wide range of porogens. Within limits, transparency is not affected by a change of cross-linker or the ratio of porogen to cross-linker in the polymerization mixture. Different polymerization temperatures, various amounts of initiator, and different porogen combinations (within limits) also left the transparency of the polymer monoliths unaffected. All these changes however caused significant changes in the morphology of the polymer.

The most dominant factor controlling transparency seems to be the refractive index of the porogen. How-

Table 8. Hg Porosimetry and N_2 Adsorption (BET) Data for Polymers IC1−IC4 (See Footnote *a* of Table 2)

polymer code	area ($m^2\ g^{-1}$)	volume ($mL\ g^{-1}$)	bulk ($g\ mL^{-1}$)	skeletal ($g\ mL^{-1}$)	*s*/*b*	pore ϕ (nm)	pore max (nm)	pore >500 nm	surf area ($m^2\ g^{-1}$)
IC1	107.0	0.38	0.82	1.18	1.45	8.0	13/40/500	yes	322
IC2	66.3	0.24	0.87	1.23	1.41	8.3	13/60/500	yes	327
IC3	95.1	0.33	0.87	1.23	1.41	7.7	13/50/500	yes	nd
IC4	100.3	0.28	0.85	1.11	1.31	7.5	13/30/200	no	456

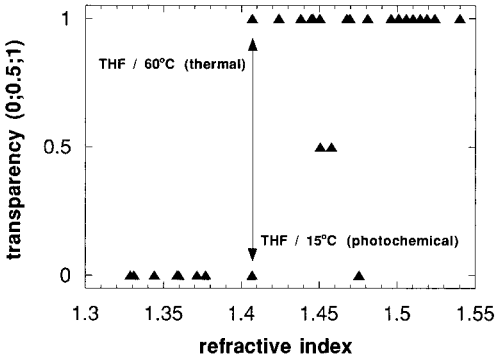

Figure 8. Plot of refractive indices of the porogens used versus the transparency of the corresponding polymer monoliths (polymers T1−T19 and S1−S9 and data taken from refs 30 and 31).

Scheme 1. Effect of Solvent Exchange on the Transparency of Polymer T19 (E1)

Solvent	*$CHCl_3$/NMP*	3 days ⟹ solvent exchange	*n-hexane*	2 days ⟹ solvent exchange	*$CHCl_3$*	2 days ⟹ solvent exchange	*methanol*
Transparency	*transparent*		*slightly milky*		*transparent*		*transparent*
Colour	*orange*		*orange*		*orange*		*dark orange*

ever, simple correlations between the porosimetry parameters of the polymer networks and the properties of the porogen have not been established. It was hoped that the pore size distribution data would correlate with polymer transparency. However, this analysis has revealed that the volume contribution of pore sizes between 1000 and 100 nm is not more than 13% of the total pore volume and this result is independent of the polymer being transparent or opaque. The fraction of pores that would scatter light therefore seems too small to affect turbidity in any significant manner.

In Figure 8 results from different investigations[30,31] together with the results described in this paper are combined. Transparency is plotted against refractive index and it is obvious that the relationship shown is not straightforward. The graph suggests that a threshold value exists, with exceptions, which separates transparent from opaque polymers. The number of exceptions, however, indicates that transparency is controlled by more than one parameter.

In particular, the morphology of the polymer also seems to be significant, as the outcome of an identical polymerization at two different temperatures demonstrates. Transparency restoration studies have indicated that a change of porogen (solvent) which differs by almost 0.1 unit in its refractive index from the original porogen is still capable of preserving the transparent state. Scattering theory predicts that a mismatch in refractive indices of 0.1, where the scatterers (polymer particles or pores) are of comparable size to the wavelength of light, would lead to a reduction in transmission of 10%.[33] Smaller or larger polymer particles will scatter less. These results indicate that the effect of the porogen on the transparency of the polymer samples is just within the prediction made. PMMA for example is considered to be transparent only when more than 90% of light is passing through the sample. As shown before, not all of the evidence can be explained by considering the influence of the refractive index. Both, refractive index and polymer morphology, have to be taken into account.

If one assumes that the transparency phenomenon encountered can be described within the classical theory of light interacting with matter, either the porogen must have the ability to form a homogeneous polymer gel or the polymer gel is only partially penetrated by the porogen but the domain sizes of the regions from which the porogen remains excluded are too small or too large to scatter light. Because no evidence was found in our investigation of a sufficient number of pores that are similar in size to the wavelength of light, one has to explain the presence of opaque polymers by assuming the presence of agglomerates of smaller pores, not detectable by nitrogen adsorption or mercury porosimetry as such, but nonetheless of sufficient size to cause significant scatter of light. This structural hypothesis is supported by a recent paper by Righetti et al.,[37] who interpreted the dependence of the transparency of their cross-linked acrylamide gels in terms of different degrees of agglomeration depending on the polymerization temperature. The direct measurement of the angular dependence of the intensity of scattered light would allow a test of this hypothesis to be made.[34]

Acknowledgment. We acknowledge receipt of a research assistantship for J.H.G.S. from the then SERC.

References and Notes

(1) Vantent, A.; Nijenhuis, K. T. *Prog. Org. Coat.* **1992**, *20*, 459.
(2) Yamaguchi, R.; Sato, S. *Liq. Cryst.* **1993**, *14*, 929.
(3) Biangardi, H. J.; Sturm, H.; Kostersitz, G. *Angew. Makromol. Chem.* **1990**, *183*, 221.
(4) Tillotson, T. M.; Hrubesh, L. W. *J. Non-Cryst. Solids* **1992**, *145*, 44.
(5) Seitz, W. R. *Anal. Chem.* **1984**, *56*, 16A.
(6) Novak, B. M.; Auerbach, D.; Verrier, C. *Chem. Mater.* **1994**, *6*, 282.
(7) Macedo, M. A.; Dallantonia, L. H.; Valla, B.; Aegerter, M. A. *J. Non-Cryst. Solids* **1992**, *147*, 792.
(8) Yamazaki, I.; Ohta, N. *Pure Appl. Chem.* **1995**, *67*, 209.
(9) Greenham, N. C.; Moratti, S. C.; Bradley, D. D. C.; Friend, R. H.; Holmes, A. B. *Nature* **1993**, *28*, 4607.
(10) Kim, D. U.; Tsutsui, T.; Sautio, S. *Polymer* **1995**, *36*, 2481.
(11) Chang, S. J.; Chiao, S.; Lai, W. J.; Lin, C. M.; Fuh, A. Y. G. *Macromol. Symp.* **1994**, *84*, 159.
(12) Janata, J. *Anal. Chem.* **1990**, *62*, 33R.
(13) Hench, L. L.; West, J. K. *Chem. Rev.* **1990**, *90*, 33.
(14) Klein, L. C. *Annu. Rev. Mater. Sci.* **1993**, *23*, 437.
(15) *ACS Symp. Ser.* **1994**, *No. 572* (all chapters).
(16) Hainey, P.; Huxham, I. M.; Rowatt, B.; Sherrington, D. C. *Macromolecules* **1991**, *24*, 117.
(17) Steinke, J. H. G.; Dunkin, I. R.; Sherrington, D. C., unpublished results.
(18) Turro, N. J.; Barton, J. K.; Tomalia, D. A. *Acc. Chem. Res.* **1991**, *24*, 332.
(19) Svec, F.; Frechet, J. M. J. *Anal. Chem.* **1992**, *64*, 820.
(20) Bradley, J.-C.; Durst, T. *Tetrahedron Lett.* **1992**, *33*, 7733.
(21) Ilg, M.; Maierrosenkranz, J.; Muller, W.; Albert, K.; Bayer, E.; Hopfel, D. *J. Magn. Reson.* **1992**, *92*, 335.
(22) Steinke, J. H. G.; Dunkin, I. R.; Sherrington, D. C. *Macromolecules* **1996**, *29*, 407.
(23) Rootare, H. M.; Frenzlow, C. F. *J. Phys. Chem.* **1967**, *71*, 2733.

(24) Brunauer, S.; Emmett, Ph.; Teller, E. *J. Am. Chem. Soc.* **1938**, *60*, 309.
(25) Hjertberg, T.; Hargitai, T.; Reinholdsson, P. *Macromolecules* **1990**, *23*, 3080.
(26) Damen, J.; Neckers, D. C. *J. Am. Chem. Soc.* **1980**, *102*, 3265. Damen, J.; Neckers, D. C. *J. Org. Chem.* **1980**, *45*, 1382.
(27) Wulff, G.; Kirstein, G. *Angew. Chem., Int. Ed. Engl.* **1990**, *29*, 684.
(28) O'Shannessy, D. J.; Ekberg, B.; Mosbach, K. *Anal. Biochem.* **1989**, *177*, 144.
(29) Shea, K. J.; Stoddard, G. J.; Shavelle, D. M.; Walmi, F.; Choate, M. M. *Macromolecules* **1990**, *23*, 4497.
(30) Rosenberg, J.-E.; Flodin, P. *Macromolecules* **1987**, *20*, 1518. Rosenberg, J.-E.; Flodin, P. *Macromolecules* **1986**, *19*, 1543.
(31) Sellergren, B.; Shea, K. J. *J. Chromatogr.* **1993**, *635*, 31.
(32) Mie, G. *Ann. Phys.* **1908**, *25*, 377.
(33) Conaghan, B. F.; Rosen, S. L. *Polym. Eng. Sci.* **1972**, *12*, 134.
(34) Willmouth, F. M. In *Optical Properties of Polymers*; Meeten, G. H., Ed.; Elsevier: Amsterdam, 1986; Chapter 5.
(35) Schmid, A.; Kulin, L.-I.; Flodin, P. *Makromol Chem., Macromol. Chem. Phys.* **1991**, *192*, 1223.
(36) Millar, J. R.; Smith, D. G.; Kressman, T. R. E. *J. Chem. Soc.* **1967**, *63*, 218. Millar, J. R.; Smith, D. G.; Kressman, T. R. E. *J. Chem. Soc.* **1965**, *61*, 304.
(37) Righetti, P. G.; Caglio, S. *Electrophoresis* **1993**, *14*, 573.

MA951875E